

11-2-2011

ALOS/PALSAR Image Processing Using Dinsar and Log Ratio for Flood Early Detection in Jakarta Based on Land Subsidences

Dodi Sudiana

Department of Electrical Engineering, Faculty of Engineering, Universitas Indonesia, Depok 16424, Indonesia, dodi.sudiana@ui.ac.id

Mia Rizkinia

Department of Electrical Engineering, Faculty of Engineering, Universitas Indonesia, Depok 16424, Indonesia

Follow this and additional works at: <https://scholarhub.ui.ac.id/mjt>



Part of the [Chemical Engineering Commons](#), [Civil Engineering Commons](#), [Computer Engineering Commons](#), [Electrical and Electronics Commons](#), [Metallurgy Commons](#), [Ocean Engineering Commons](#), and the [Structural Engineering Commons](#)

Recommended Citation

Sudiana, Dodi and Rizkinia, Mia (2011) "ALOS/PALSAR Image Processing Using Dinsar and Log Ratio for Flood Early Detection in Jakarta Based on Land Subsidences," *Makara Journal of Technology*: Vol. 15 : No. 2 , Article 15.

DOI: 10.7454/mst.v15i2.940

Available at: <https://scholarhub.ui.ac.id/mjt/vol15/iss2/15>

This Article is brought to you for free and open access by the Universitas Indonesia at UI Scholars Hub. It has been accepted for inclusion in Makara Journal of Technology by an authorized editor of UI Scholars Hub.

ALOS/PALSAR IMAGE PROCESSING USING DINSAR AND LOG RATIO FOR FLOOD EARLY DETECTION IN JAKARTA BASED ON LAND SUBSIDENCE

Dodi Sudiana^{*)} and Mia Rizkinia

Department of Electrical Engineering, Faculty of Engineering, Universitas Indonesia, Depok 16424, Indonesia

^{*)}E-mail: dodi.sudiana@ui.ac.id

Abstract

Flood that occurred in Jakarta is not only influenced by rainfall, urban planning system and drainage alone, but also may be involved land subsidence (LS). LS is possible in because Jakarta stands on top of layers of sediments and the presence of ground water consumption in very large quantities. In this research, the Advanced Land Observing Satellite (ALOS)/Phased Array type L-band Synthetic Aperture Radar (PALSAR) data was processed to determine the level of LS in Jakarta area and its relation to flood potential area. Differential interferometry method (DInSAR) was performed on two PALSAR data with different acquisition years, i.e. 2007 and 2008, respectively. DInSAR processing generated images containing information that can be converted into LS. To find the elevation changing area, log ratio algorithm was applied to those images as the additional analysis. The log ratio image is superimposed on the DInSAR result and Jakarta inundation map of 2009, to acquire the relationship between LS and the flood and flood vulnerability map of Jakarta based on LS. It is found that lands on the flooded area of 10.57 cm on the average, with a minimum and maximum of 5.25 cm and 22.5 cm, respectively. The greater the value of LS, inundation area also tend to widen, except in a few areas that have special conditions, such as reservoirs, river flow solution, water pump system and sluices. Accuracy of DInSAR result image is quite high, with the difference of 0.03 cm (0.18%) to 0.55 cm (3.37%) as compared to those from GPS measurements. These results can be recommended to the local government of Jakarta to minimize the potential risk of flood, as well as the subject of city planning for the future.

Keywords: ALOS/PALSAR, DInSAR, flood potential area, land subsidence (LS), log ratio

1. Introduction

Jakarta is one of the capital cities that frequently suffer from flash flood in the world. The location of Jakarta which stands on sediment layer and crossed by Ciliwung River and its tributaries cause this disaster. This condition leads to land subsidence (LS) since most skyscrapers, offices and housings have drained ground water in large numbers in spite of city rapid development. Remote sensing and Geographic Information System (GIS) methods have been used to analyze land phenomena, such as land subsidence (LS) using the difference of ground level [1]. LS phenomenon can be viewed as one factor and also a parameter indication of flooding in a specific region. LS has been investigated from SAR (Synthetic Aperture Radar) data using Interferometry Approach (InSAR) in China [2], in mountain slopes [3] and geothermal field [4], while Permanent Scatter (PS) InSAR is applied in [5-6]. Investigation the correlation LS to high water-pumping rate is reported in [7-8]. Using Differential Interferometry Approach (DInSAR), LS for the area of

New Orleans and Louisiana (United States) [9], Bologna, Mexico City [10], Kalkota, India [11], Burgan field of Kuwait [12], Granada, Spain [13], and Semarang, Indonesia [14-15] were investigated. Due to excessive pumping of groundwater, study of subsidence phenomena using advance DInSAR-Coherent Pixels Technique (CPT) is investigated in [16-17]. DInSAR is compared with classical change detection approach using the Mean Ratio Detector (MRD). Where in [14], interferometry is performed using Multiple Acquisition Radar Interferometry (MARI) method which had the same principle with DInSAR. Advanced DInSAR technique, referred to as DInSAR-SBAS (Small Baseline Subset) has been applied to study the surface deformations in sedimentary basin [18]. DInSAR has an advantage that the number of SAR images required is less with the acquisition of spatially point diversified. It also shows a good level of coherency on the entire set of interferogram [19]. Interferometry generated by a PALSAR L-band data also has an advantage related to phase unwrapping which often to be a problem in SAR interferometry data in C-band wavelength like European

Remote Sensing Satellite (ERS). Interferometry of L-band SAR is an appropriate method to monitor the LS in Japan [20]. The goal of this research is producing a map of flooding potential areas by using radar data retrieved from ALOS/PALSAR for Jakarta based on the LS. The results are expected to be used as recommendations for flood prevention action and planning, implementation, and controlling of sustainable urban development. The input data from ALOS/PALSAR and digital elevation model (DEM) from the Shuttle Radar Topography Mission (SRTM) are used to analyze the LS. The output of this research is Jakarta flood vulnerability map based on the LS.

2. Methods

To achieve the relationship between LS and flooding potential area, we overlaid three images. The first image is the image processing of DInSAR from two Level 1.0 PALSAR data which cover Jakarta region in different acquisition years (2007 and 2008, respectively). Each intensity of the image pixel is represented in RGB, containing a correlation with phase change. The value of phase change was then converted to an altitude. Thus, from this process, the height change of each pixel could be derived.

The second layer is the image from processing of two data using the Log Ratio method. This method could be used to detect land elevation changes by involving statistical values of the image histogram. The results are black and white images which define the area of changes. The third layer is a flooding/inundation map of Jakarta in 2008. All data were processed and analyzed systematically as shown in Fig. 1.

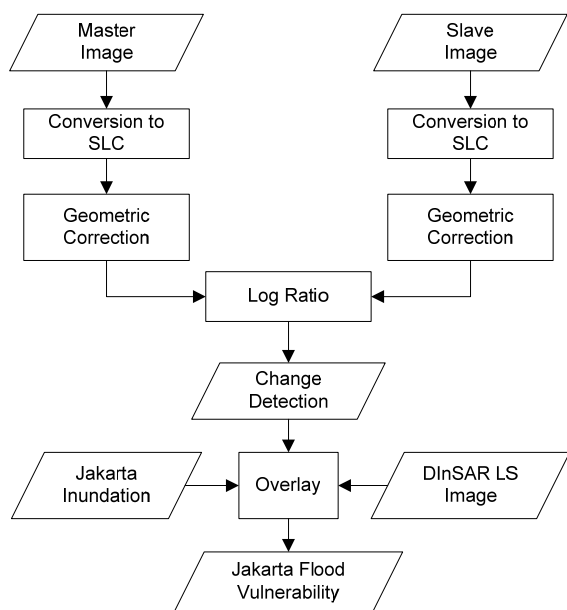


Figure 1. Flowchart of Data Processing ALOS/PALSAR for Jakarta Flood Vulnerability Map

Master and slave images are PALSAR imageries which were taken before and after flooding, respectively, were converted into single look complex (SLC) data. Since the satellite data has disturbed due to satellite height, rotation and roundness of the Earth, it has to be corrected geometrically based on real geographic positions in the surface. Two methods were applied to retrieve the elevation changes using Log ratio and DInSAR, respectively. Log ratio method was implemented to observe where elevation changes occurred, while DInSAR was used to generate the LS map. These results along with the Jakarta flooding map were then overlaid to derive the flood vulnerability map.

Change detection using log ratio method.

Rationalization method minimizes more errors in image regions with high intensity, rather than pixel-per-pixel difference that reduces the image intensity values. This method is logical since rationalization involves mean and variance of image histogram, which covers the overall pixel values. The log ratio process begins by calculating log ratio detector as the logarithm of the average intensity ratio [21].

If there are two SAR images, $I_1 = \{I_1(i, j), 1 \leq i \leq nrows, 1 \leq j \leq ncolums\}$ and $I_2 = \{I_2(i, j), 1 \leq i \leq nrows, 1 \leq j \leq ncolums\}$, thus the *log ratio detector* is defined by [21] as formulated in Eq. (1).

$$I_{LR} = \left[\frac{\sum_{(k,l) \in V_{ij}} I_2(k,l)}{\sum_{(k,l) \in V_{ij}} I_1(k,l)} \right] \tag{1}$$

where V_{ij} is a neighbour pixels (i, j) in [19].

For distinguishing the changed region (c) from the unchanged (u), a threshold selection criteria is needed. Assuming that c and u in the image ratio (the log ratio results) represented two opposite classes, the minimum error threshold or also called threshold selection criteria Kittler Illingworth (KI) [22], is derived from the assumption that the object and background are normally distributed. KI method is based on Bayesian decision theory and requires a parametric model to describe the statistical distribution for the region that has changed or not [21].

If each of the two components is normally distributed, the criterion function of the KI method is formulated in Eq. (2).

$$J(T) = 1 + 2 \left[P_1(T) \log \sigma_1(T) + P_2(T) \log \sigma_2(T) \right] - 2 \left[P_1(T) \log P_1(T) + P_2(T) \log P_2(T) \right] \tag{2}$$

Above parameters can be calculated by Eqs. (3) and (4).

$$P_u(T) = \sum_{g=0}^T H(g) \quad \mu_u = \frac{1}{P_u(T)} \sum_{g=0}^T H(g)g \tag{3}$$

$$\sigma_u^2 = \frac{1}{P_u(T)} \sum_{g=T+1}^T [g - \mu_u(T)]^2 hH(g)$$

$$P_c(T) = \frac{1}{\sum_{g=T+1}^{L-1} H(g)} \quad \mu_c = \frac{1}{P_c(T)} \sum_{g=T+1}^{L-1} H(g)g \quad (4)$$

$$\sigma_c^2 = \frac{1}{P_c(T)} \sum_{g=T+1}^{L-1} [g - \mu_u(T)]^2 H(g)$$

where $H(g)$ ($g = 0, 1, \dots, L-1$) is a histogram of the log ratio image. $\mu_i(T)$ ($i = u, c$) is the average value of the class c (changed) and u (unchanged). $\sigma_i^2(T)$ ($i = u, c$) are the variance of both classes. Optimal threshold that minimizes the error is minimized by the function which has the criteria expressed in Eq. (5).

$$T^* = \arg \min_{0 \leq T \leq L} J(T) \quad (5)$$

Change detection algorithm using log ratio method is intended to help the analysis process by localizing the area of observation height change from PALSAR image. This method was applied to both of PALSAR image that has been reconstructed in Single Look Complex (SLC) data. The final step is to compose a color composite image for visualization the phase difference. Basic reduction formula was implemented to retrieve the information value of pixels and phase difference is was converted to height difference.

The colors in the image DInSAR results represent different heights. For a single phase cycle, it represents 2π (pi), where 2π (pi) represents the half of wavelength. Since the wavelength of L-band PALSAR type is 24 cm, a cycle in the image DInSAR could be projected as 12 cm in height.

DInSAR Process. To generate Jakarta Flood Potential Map, we process the ALOS/PALSAR data using DInSAR algorithm to generate DInSAR image for land subsidence, which is systematically shown in Fig. 2.

The software used for the initial process is PALSAR Processor 2.6.3 and PALSAR Fringe 4.5.1. The earlier software is used to process PALSAR data to retrieve the interferometry. The latter one is then executed to achieve the fringe and color composite which is converted to height.

Jakarta Inundation Map. The flooding map used in the analysis is Jakarta's 2009 flood inundation map, when the flooding occurred after the time of satellite observation. This map is used to find slices of land subsidence area and flooding area, so the relationship between the land subsidence and the flooding area could be analyzed. Incision was done by overlaying images which is necessary. This map also provides altitude pool information. The registration process of master and slave image, cropping area of Jakarta, the log ratio process and log ratio image overlays with DInSAR were performed using graphics processing software. Furthermore, to facilitate spatial analysis of other data (maps of watershed and municipality boundaries), we used open source software Google Earth.

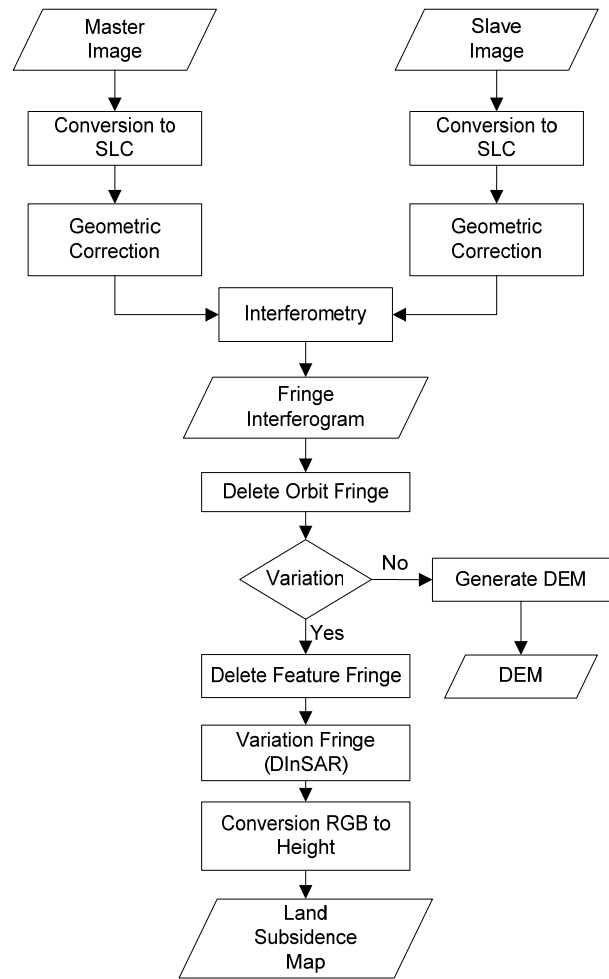


Figure 2. Flowchart of ALOS/PALSAR Data Processing for DInSAR Process

3. Results and Discussion

Data Overlay. After making the incision between DInSAR image and log ratio image, the data is presented on a spatial map from Google Earth, and overlaid with a map pool. The analysis results showed a polygon inundation as many as 27 regions spread across the five municipalities in Jakarta as shown in Fig. 3. Some of these area showed land subsidence within the polygon of each flooding area. The resulting data accumulated that the average subsidence is 10.57 cm in the inundation area.

Within the entire flooding area, it is obtained that the minimum and maximum value of land subsidence is 5.25 cm and 22.5 cm, respectively; with average of 10.57 cm. Tegal Alur (region A) experienced the highest land subsidence of the entire existing inundation polygons (22.5 cm). Furthermore, a significant subsidence occurred in Pluit (C, 21 cm) and Penjaringan (D, 16.5 cm). Description of the LS and the height of inundation are shown graphically in Fig.4.

The LS value of Tegal Alur (region A) is seen having a correlation with its height of inundation. Among the neighbor regions (A-F), Tegal Alur has the highest LS value and also the greatest value of floodwaters inundation. While Pluit and Penjaringan (C, D), despite having a fairly large LS value, the floodwater

inundations that occurred were fairly low compared to Kapuk Muara (B), Semanan (E) and Rawa Buaya (F). This could be caused by the existence of dam built by housing developers and government to prevent flooding, especially flood caused by sea water [23].

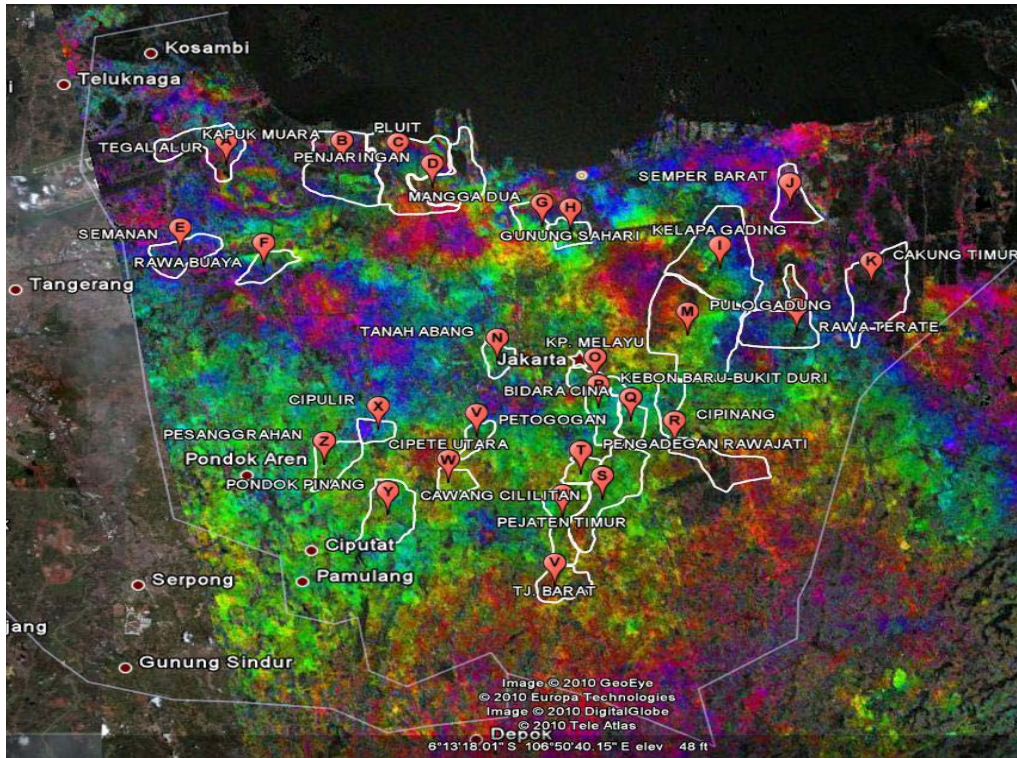


Figure 3. The Result of DInSAR Image Overlay, Log Ratio and Flood Inundation Map

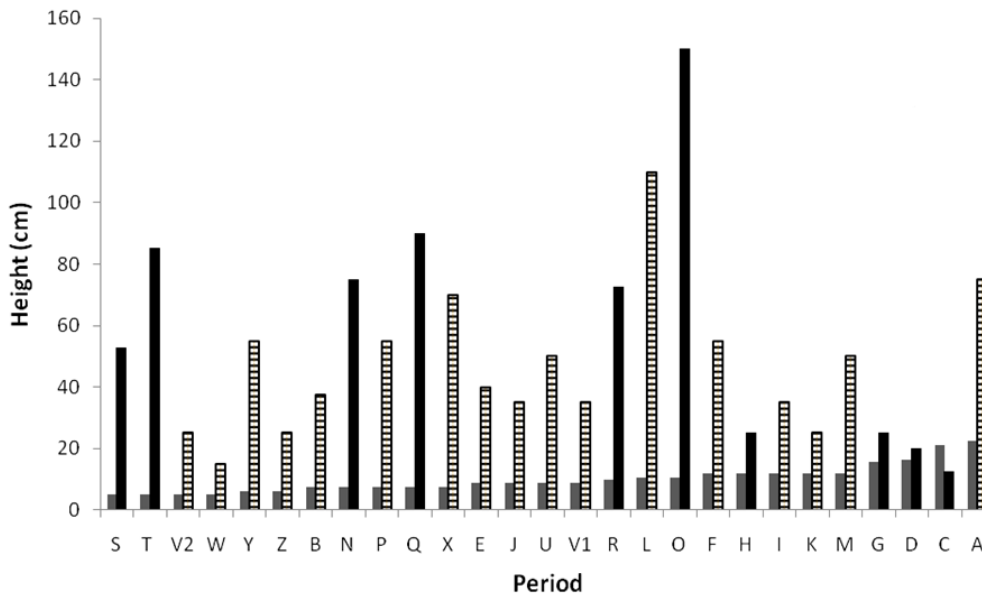


Figure 4. LS Value and the Height of Inundation for Each Region based on LS (Ascending; ■), Inundation (▨), Exception (External Factor; ■)

Furthermore, Mangga Dua and Gunung Sahari (G and H regions), which are known as trading area, experienced LS above the average value. This could be caused by fast development of buildings, considering this region as rapid growing trading area. But the flooding level is low enough (<30 cm). This could be caused by river flow furcation since the flow of Ciliwung River along Gunung Sahari street is partially divided into namely towards Ciliwung River through Hayam Wuruk/Gajah Mada street and the rest headed Pekapuran sluice, Ancol before heading to sea. The point of flow breaking is Jembatan Merah sluice in Mangga Besar in the northeast area of Jakarta, which is represented by a polygon I-N, LS that occurred was still in the range of average value. From the DInSAR image, it is seen that one cycle of phase occurred in Kelapa Gading (I), Cakung Timur (K), and Pulogadung (M), which means the LS value is half of the wavelength of PALSAR, i.e. 12 cm. Most of these areas are still experiencing flood elevation in medium level. This is in line with LS value which is around the average value. Fairly extreme values occurred in area of Rawa Ternate (L), Pulogadung (M) and Tanah Abang (N), which experienced quite high inundation of flood. Rawa Ternate and Pulogadung regions are industrial area in Jakarta. This type of land use caused land subsidence related to the fast growing in number and magnitude of permanent buildings standing on it. Change in land use in an area also becomes one of the factors causing flood in Jakarta. Therefore, the density of industry in these two regions is analyzed as the cause of flood inundates. Because of that reason, the government is building Banjir Kanal Timur project as a solution to the northeast flood region in Jakarta.

While in Tanah Abang area which has high inundation, the LS is low since the policy of SDPU-DKI in preventing flood is employed in the vital areas around Merdeka Barat, namely by retaining as much as possible flood water of Banjir Kanal at Karet sluice. Therefore, the flood occurred in Jati Pinggir-Tanah Abang and Kebon Kacang [24].

In the area of high dense industrial and government buildings, LS occurred due to the burden of building, besides the sediment layers at the bottom of Jakarta. The burden of building represents the load of building pressure in large quantities and more permanent.

In the south area of Jakarta, LS was below the average. The greatest value of LS occurred in Kampung Melayu (O region, 10.5 cm) and Cipinang (R, 10 cm). However, these two regions experienced the highest inundation of floodwaters besides Kebon Baru and Bukit Duri (Q) that are located in Ciliwung River flowing area through Kampung Melayu. The high inundation in this area is not comparable to the LS value since this area is crossed by the Ciliwung River before it is splitted into two

streams in Manggarai sluice. Meanwhile, if the water discharge is high, water will flow through this area first before Manggarai sluice. The operation of Manggarai sluice (open-close) is also associated to the policy of securing government area from the floodwaters. Therefore, these regions are very likely to experience high inundation.

Compared with ground survey that is already investigated in [23] using GPS, there are three common observations with the 27 locations which are investigated in this research, as shown in Table 1 and Fig. 5. The minimum and maximum differences between ground survey and our result are 0.03 cm and 0.55 cm, respectively. Differences may occur due to the wavelength rounded of PALSAR from 23.5 cm to 24 cm in the PALSAR Processor software. From these results, it could be concluded that the detection of LS value using DInSAR method is quite accurate.

Prediction of Flood Potential Area based on LS.

Based on analysis of DInSAR and inundation map, it is identified that the average LS in flooded area measured as deep as 10.57 cm. With these results, we analyze the flood control area and watershed, which are then transformed into flood potency map based on the LS as shown in Fig. 6. In the Figure, flood potential zones are indicated by red and yellow polygons. Red polygon indicates the potential flood area that has experienced flood in January 2009, while yellow polygons cover the area with LS value above the average. These zones are also generated from the analysis of watershed and flood control. The detail area of these regions are shown in Table 2.

Table 1. Comparison of DInSAR and GPS Measurement (January 2007-November 2008)

Location	Land Use [24]	Region	GPS (cm)	DInSAR (cm)	Difference
Mutiara	Settlements, ports, recreation area	D (Penjaringan)	16.47	1.50	0.03 cm (0.18%)
Glodok	Trading	G (Mangga Dua)	16.3	15.75	0.55 cm (3.37%)
Cakung	Industry	K (Cakung)	11.5	12.00	0.50 cm (4.35%)

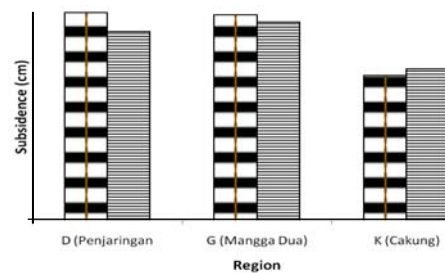


Figure 5. Comparison of DInSAR and GPS Measurement

Based on the LS values in these seven regions shown in the Table, the smallest flood potential is located in the southeast area of Jakarta, namely the district of Ciracas, Cipayung, Cijantung and Pasar Rebo. And the most potential area is in the eastern Jakarta, namely in district of Rawamangun, Cempaka Putih and Cakung, including Pulogadung, which is located further to the north but is still covered in this area. These results are quite appropriate compared to 2007 Jakarta's Map Projections Floods as shown in Fig. 7. This map is produced by Jakarta Public Work Department after 2007 flood which is one of flash floods in Jakarta, since the enormous flood in 2002. In this map, the area that did not experience flood on January 16, 2009, become flooding area. The areas in questions include Cipayung, Ciracas, Kebon Jeruk, Cilandak and Kalideres. These regions are also detected as flood potential area based on the LS analysis.

By monitoring the value of land subsidence in Jakarta using DInSAR method from year to year, the trend of land subsidence could be estimated. Moreover, it is expected to be one of important consideration for future Jakarta city planning.

Table 2. LS Values of Jakarta Flood Prediction Area

Label	Area	LS (cm)
1	Pegadungan, Kalideres, Kapuk	15.75
2	Mangga dua, Ancol, Pademangan	12.00
3	Rawamangun, Cempaka Putih, Cakung	27.00
4	Kebon Jeruk, Kemanggisan, Rawa Buaya, Semanan	12.00
5	Manggarai, Bukit Duri, Karet, Menteng	12.00
6	Ciracas, Cipayung, Cijantung, Pasar Rebo	10.50
7	Cilandak	12.00

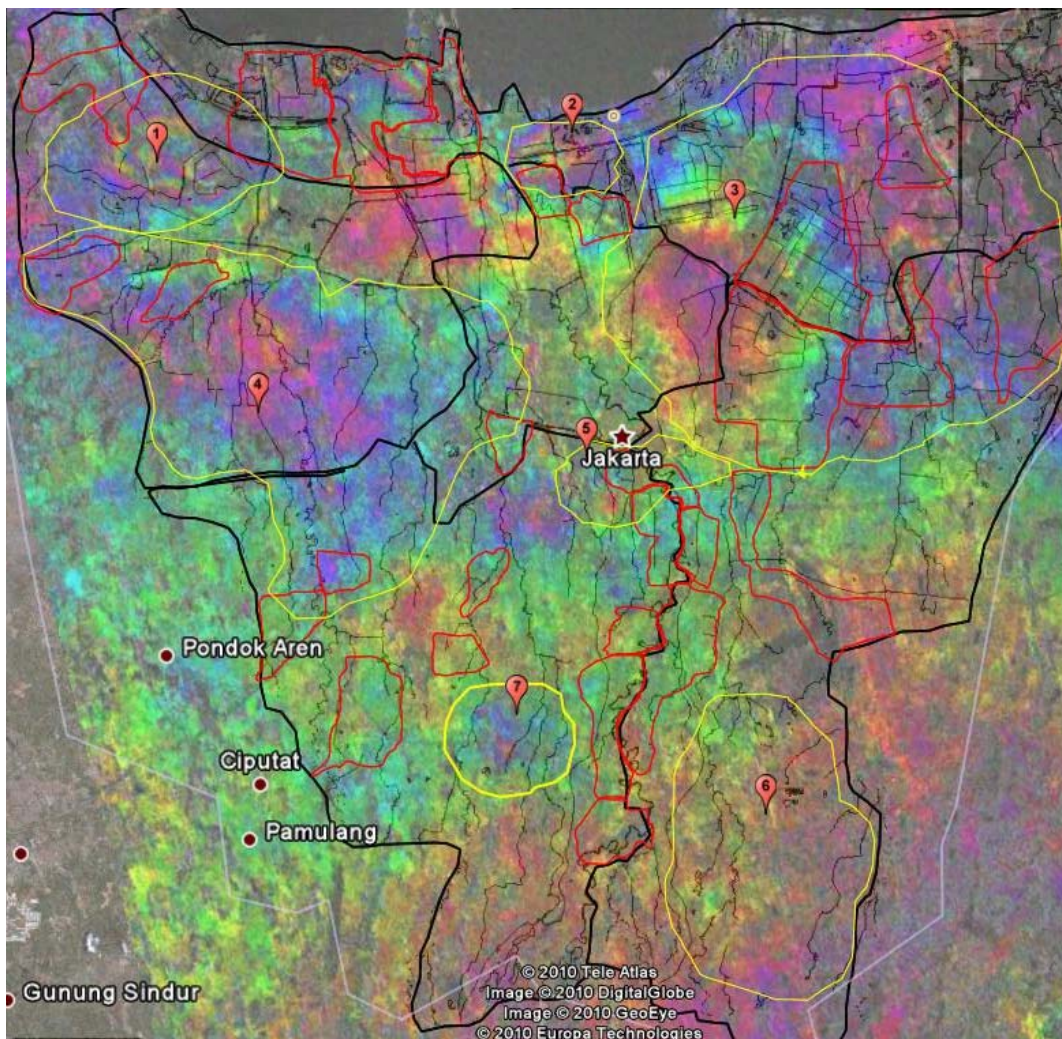


Figure 6. Jakarta Flood Potency Map based on the LS

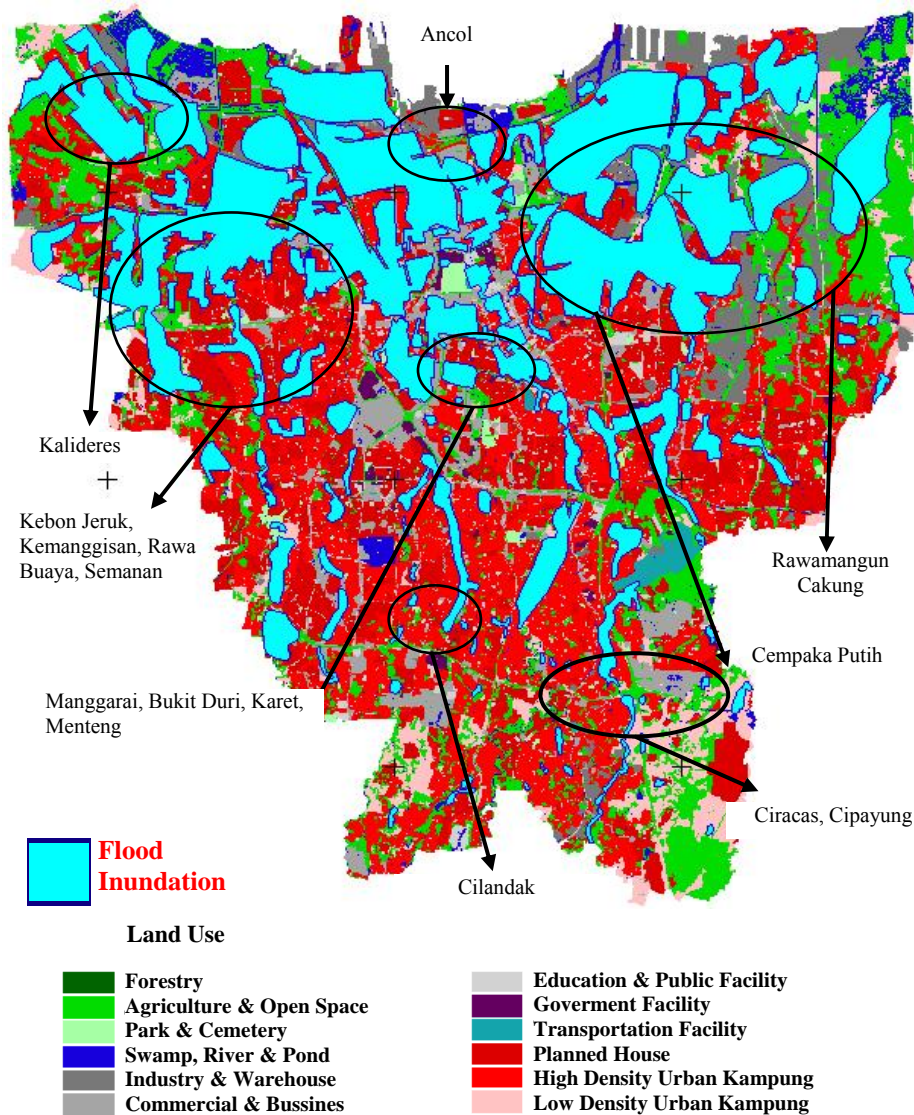


Figure 7. Jakarta Flood Projection Map in 2007 [25]

4. Conclusion

Flood that occurred in Jakarta is also influenced by Land Subsidence (LS). LS value that retrieved from ALOS/PALSAR data using DInSAR method on January 2007 and November 2008 in Jakarta flooding area ranged from 5.25 cm to 22.5 cm with average of 10.57 cm. The highest LS found in Tegal Alur, Pluit and Penjaringan districts. Some regions that were not flooded in January 2009 have the possibility of flooding, which are noted to have high LS such as Cipayung, Ciracas, Kebon Jeruk, Cilandak and Kalideres districts. High LS regions which had not shown flood are identified as regions having flood control policy regulated by the Government (such as usage of reservoirs, pumps, water breaking). Deriving LS values using DInSAR method provided evidence of high accuracy, which differences to GPS measurements

ranges from 0.03 cm (0.18%) to 0.55 cm (3.37%). By monitoring LS of Jakarta from year to year, the subsidence trends could be predicted and is expected to be considered in future city planning.

Acknowledgment

The authors would like to thank the Microwave Remote Sensing Laboratory (MRSL), Center for Environmental Remote Sensing (CEReS), Chiba University for providing the ALOS/PALSAR images used in this work under the International Collaboration Project funded by the DGHE; and Ministry of National Education and the RUUI Research Grant from Universitas Indonesia under contract No. 2584/H2.R12/PPM.00.01 Sumber Pdanaan/2010 for the financial support to the research.

References

- [1] B.M. Sukojo, D. Susilowati, Makara Teknologi 7/1 (2003) 1.
- [2] C.Y. Zhao, Q. Zhang, X.L. Ding, Z. Lu, C.S. Yang, X.M. Qi, Environm. Earth Sci. 58/7 (2009) 1533.
- [3] H. Rott, T. Nagler, Adv. in Space Res. 37/4 (2006) 710.
- [4] J.K. Hole, C.J. Bromley, N.F. Stevens, G. Wadge, J. of Volc. and Geoth. Res. 166/3-4 (2007) 125.
- [5] C. Colesanti, J. Wasowski, Eng. Geology 88/3-4 (2006) 173.
- [6] Y. Guoqing, M. Jingqin, Earth Sci. Frontiers 15/4 (2008) 239.
- [7] C.P. Chang, T.Y. Chang, C.T. Wang, C.H. Kuo, K.S. Chen, Math. and Comp. in Simulation, 67/4-5 (2004) 351.
- [8] B. Osmanoglu, T.H. Dixon, S. Wdowinski, E. Cabral-Cano, Y. Jiang, Int. J. of Appl. Earth Obs. and Geoinf. 13/1 (2011) 1.
- [9] V.V. Chamundeeswari, D. Singh, K. Singh, W. Wiesbeck, IGARSS Proc. (2008) IV-518.
- [10] T. Strozzi, U. Wegmüller, C.L. Werner, A. Wiesmann, V. Spreckels, IEEE Trans. on Geosc. and Rem. Sens. 4/7 (2003) 1702.
- [11] R.S. Chatterjee, B. Fruneau, J.P. Rudant, P.S. Roy, P.-L. Frison, R.C. Lakhera, V.K. Dadhwal, R. Saha, Rem. Sens. of Environm. 102/1-2 (2006) 176.
- [12] Saifuddin, A. Al-Dousari, A. Al-Ghadban, M. Aritoshi, J. of Petrol. Sci. & Eng., 50/1 (2006) 1.
- [13] P. Fernandez, C. Irigaray, J. Jimenez, R. El Hamdouni, M. Crosetto, O. Monserrat, J. Chacon, Eng. Geology 105/1-2 (2009) 84.
- [14] A.M. Lubis, T. Sato, I. Nobuhiro, N. Tomiyama, T. Yamanokuchi, Rem. Sens. Tech. Center of Japan, 2009.
- [15] A.M. Lubis, T. Sato, N. Tomiyama, N. Isezaki, T. Yamanokuchi, J. of Asian Earth Sci. 40/5 (2011) 1079.
- [16] R. Tomás, Y. Márquez, J.M. Lopez-Sanchez, J. Delgado, P. Blanco, J.J. Mallorquí, M. Martínez, G. Herrera, J. Mulas, Rem. Sens. of Environm. 98/2-3 (2005) 269.
- [17] G. Herrera, R. Tomás, D. Monells, G. Centolanza, J.J. Mallorquí, F. Vicente, V.D. Navarro, J.M. Lopez-Sanchez, M. Sanabria, M. Cano, J. Mulas, Eng. Geology 116/3-4 (2010) 284.
- [18] S. Stramondo, M. Saroli, C. Tolomei, M. Moro, F. Doumaz, A. Pesci, F. Loddo, P. Baldi, E. Boschi, Rem. Sens. of Environm. 110/3 (2007) 304.
- [19] O. Mora, J.J. Mallorquí, J. Duro, Geosci. and Rem. Sens. Symp., IGARSS, Boston, 2002 p.2696.
- [20] S. Takeuchi, S. Yamada, Geosci. and Rem. Sens. Symp., IGARSS 4 (2002) 2379.
- [21] F. Wu, C. Wang, H. Zhang, B. Zhang, Geosci. and Rem. Sens. Symp., IGARSS, 2007, p.2601.
- [22] Y. Bazi, L. Bruzzone, F. Melgani, IEEE Trans. on Geosc. and Rem. Sens. 43/4 (2005) 874.
- [23] L. Bayuaji, J.T.S. Sumantyo, H. Kuze, The Canadian J. of Rem. Sens. 36/1 (2010) 1.
- [24] I. Riyanto, Master Thesis, Department of Electrical Engineering, Faculty of Engineering, Universitas Indonesia, Indonesia, 2009.
- [25] Dinas Pekerjaan Umum DKI Jakarta, Pedoman Pengendalian Banjir Jakarta, Dinas PU DKI Jakarta, Jakarta, 2007.